Chapter 4

Epistemic Uncertainty Quantification of Seismic Damage Assessment

Hesheng Tang, Dawei Li and Songtao Xue

Additional information is available at the end of the chapter

http://dx.doi.org/10.5772/intechopen.68153

Abstract

The damage-based structural seismic performance evaluations are widely used in seismic design and risk evaluation of civil facilities. Due to the large uncertainties rooted in this procedure, the application of damage quantification results is still a challenge for researchers and engineers. Uncertainties in damage assessment procedure are important consideration in performance evaluation and design of structures against earthquakes. Due to lack of knowledge or incomplete, inaccurate, unclear information in the modeling, simulation, and design, there are limitations in using only one framework (probability theory) to quantify uncertainty in a system because of the impreciseness of data or knowledge. In this work, a methodology based on the evidence theory is presented for quantifying the epistemic uncertainty of damage assessment procedure. The proposed methodology is applied to seismic damage assessment procedure while considering various sources of uncertainty emanating from experimental force-displacement data of reinforced concrete column. In order to alleviate the computational difficulties in the evidence theory-based uncertainty quantification analysis (UQ), a differential evolution-based computational strategy for efficient calculation of the propagated belief structure in a system with evidence theory is presented here. Finally, a seismic damage assessment example is investigated to demonstrate the effectiveness of the proposed method.

Keywords: damage model, epistemic uncertainty, uncertainty quantification, evidence theory, differential evolution algorithm

1. Introduction

With widespreading of the concept and applications of performance-based earthquake engineering (PBEE) and performance-based seismic design (PBSD), the effective measures for assessing the performance state of structural components or entire structure have been deeply

investigated in seismic engineering. In consistence with the different performance assessment criteria, the evaluation and measurements of damage states for structural components are divided into three main branches (e.g., displacement-based approach, energy-based measure and the combination of both). Due to the simplicity and convenience of observation and description for structural damage states, the displacement-based approach and corresponding damage index (e.g., inelastic displacement, maximum inter story drift ratio, and ductility demand, etc.) have been widely documented in building seismic evaluation and retrofit of existing building guidelines [1]. Notwithstanding the prevalent application of displacement method in damage assessment, the defect of lacking the influence of low cyclic fatigue of structural components is obvious. The hysteretic energy dissipation is considered as a more reasonable indicator for seismic structural damage, because it is a cumulative parameter involved cyclic-plastic deformations in a structure during earthquakes [2]. Despite the effectiveness of hysteretic energy, experimental observations demonstrate that the expression of energy would be significantly affected by the exceedance plastic deformation [3]. And the cumulative laboratory experimental data on structural members and structures indicate the fact that the structure is damaged by a combination of the excessive deformation and hysteretic energy. Park–Ang damage model [4], which takes into account the effects of both the first exceedance failure and cumulative damage failure in low-cycle-fatigue for a structural component during seismic load, is served as a baseline for many researches. Due to intrinsic simplicity as well as calibrations against a significant amount of observed seismic damages, the Park-Ang model and its modified version have been extensively implemented in seismic performance evaluation of structures [5–7].

Although the applicability and practicability of using the Park-Ang model and its modified versions have been supported by many researchers [8, 9], it should be noted that the Park-Ang-damage-index-based performance evaluation is still a challenging task due to the large uncertainties associated with the damage model parameters [10]. With the influence of these uncertainties [11, 12], the evaluation results of structural damage state are always represented with the empirical interval value (e.g., the minor damage state is represented by $0.25<D<0.4$ or $0.11<D<0.4$, etc. [13]). Some of these uncertainties stem from factors that are inherently random (or aleatory) in engineering or scientific analysis (e.g., material properties such as Young's modulus of steel; compression strength of concrete). Others arise from a lack of knowledge, ignorance, or modeling (e.g., simplification of mathematical model of buildings for structural analysis purposes). The large uncertainties associated with the Park-Ang damage model are derived from limited experimental data and approximate modeling (lack of knowledge) [2, 4, 5, 10]. Considering the importance of damage model in assessment of damage state for a structure, the epistemic uncertainty shall be taken into account in seismic damage state assessment with great care. Hence, it is significant to present a comprehensive uncertainty analysis methodology to quantify the epistemic uncertainty and obtain more reliable results.

The traditional probability theory, based on the sufficient statistical information, is used to model the objective uncertainty (random), which is inherent in physical variability of materials and environment. Unfortunately, the limited number of experimental data set cannot support the strong assumption of probability theory, and the process of collecting data is

always costly and time consuming. These shortcomings lead the assessment result of damage state of structures are not aleatory but epistemic. In the past decades, several alternative approaches have been developed to deal with epistemic uncertainty. Some of the potential uncertainty theories are the theory of fuzzy set [14], possibility theory [15], the theory of interval analysis [16], imprecise probability theory [17], and evidence theory [18, 19]. Among these promising uncertainty representation models, evidence theory with the ability of handling aleatory and epistemic uncertainty is used for UQ, risk assessment, and reliability analysis.

With two complementary measures of uncertainty such as belief and plausibility, using evidence theory to UQ is flexible and effective. In comparison with the calculation of single probability density function (PDF) in probability theory, the computationally intensive problem involves computing the bound values over all possible discontinuous sets which is a main shackle of wide application for evidence theory. In order to break the computational barriers in the evidence theory-based UQ, the differential-evolution-based interval optimization is employed to enhance the computational efficiency as described by the authors [20].

2. Sources of uncertainty in seismic damage assessment

To effectively describe the damage state of structural components or entire structure, the original Park-Ang damage model and modified model were developed. The original Park-Ang damage model was presented here to access the uncertainty influence of the evaluation on the damage state of column components. There are various methods to estimate constants in Park-Ang damage model in different studies. In addition to diverse combination measures, the empirical estimation value and calibration value dispersed in a large range. Using the classification method proposed by Oberkampf and Helton [21], the aleatory and epistemic uncertainties involved in Park-Ang damage model are listed as:

1. The random uncertainties rooted in experimental materials, e.g., the material composition of concrete and the strength test results in single compositional material.
2. The objective and subjective uncertainties of experimental condition. e.g., the environmental factor, the loading error of machine, and measurements error.
3. The subjective uncertainties of fitting measures of parameters in Park-Ang damage model and mathematical representation of model itself.

In consideration of these aleatory and epistemic uncertainties in Park-Ang damage model, the quantification influence of uncertainties is indispensable. To achieve this goal, a series of empirical expressions are summarized. Then, the Structural Performance Database of Pacific Earthquake Engineering Research Center (PEER) is used to construct the uncertain sources of parameters of damage assessment models. Using these calibration results of column set, the parameter uncertainties are represented by the fluctuation of ratio of empirical values and calibration values.

2.1. Park-Ang model and empirical expression of its constants

The Park-Ang damage model [4] combines the first exceedance failure and cumulative damage failure with a linear expression as:

$$D = \delta_m/\delta_u + \beta \int dE/F_y\delta_u \tag{1}$$

where δ_m is the maximum deformation under earthquake, δ_u is the ultimate deformation under monotonic load, $\int dE$ is the cumulative energy under earthquake, β is the energy coefficient, and F_y is the yield strength. In order to simplify the analysis procedure, the value of F_y, δ_u, and β are always assumed as the constants and have nothing to do with the loads pattern. Following above assumption, the value of damage index D for per-load stage can be computed by only using the current value of δ_m and $\int dE$. Furthermore, the damage evolution of structures and components can be described and this evolution index is supported to estimate the true damage stage of structure and components.

In the last two decades of the twentieth century, a set of experimental results were conducted and some illuminate-, empirical-, or mechanical-based expression of F_y, δ_u, and β were successively generated. Park et al. [4] computed the value of β as given in Eq. (2):

$$\beta = (-0.447 + 0.073l/d + 0.24n_0 + 0.314\rho_t) \times 0.7^{\rho_\omega} \tag{2}$$

where l and d denote the length span and effective height of cross section, n_0 is the axial load ratio, ρ_t is the longitude tension steel ratio (%), and ρ_w is the confinement ratio (%). Kunnath et al. [5] used 260 beams and columns data to fit the value of β as given in Eq. (3):

$$\beta = [0.37n_0 + 0.36(k_p - 0.2)^2]0.9^{p_w} \tag{3}$$

where $k_p = \rho_t f_y/0.85f_c$ is normalized steel ratio and ρ_w is confinement ratio. Similarly, δ_u can be determined with statistical approach or fundamental method using the mechanics of concrete and steel. Using the typical statistical measure, Park [6] evaluated the ultimate displacement as:

$$\delta_u = 0.52(l/d)^{0.93}\rho^{-0.27}\rho_\omega^{0.48}n_0^{-0.48}f_c^{-0.15} \times \delta_y \tag{4}$$

where ρ is normalized steel ratio and δ_y is the yield displacement of components that can be computed with [4] and other factors are same as above. Compared to above statistical calculation model, EU 8 [22] and Fardis and Biskinis [23] presented two different models with the mechanics of concrete and steel:

$$\delta_u = \frac{1}{\gamma_{el}}0.016(0.3)^{n_0}\left[\frac{\max(0.01,\omega')}{\max(0.01,\omega)}f_c\right]^{0.225}\left[\min\left(9,\frac{l}{h}\right)\right]^{0.35}25^{\left(\alpha\rho_{sx}\frac{f_{yw}}{f_c}\right)} \times l \tag{5}$$

$$\delta_u = \alpha_{st}(1 - 0.4\alpha_{cyc})(1 + 0.5\alpha_{sl})(0.3)^{n_0}\left[\frac{\max(0.01,\omega')}{\max(0.01,\omega)}f_c\right]^{0.175}\left(\frac{l}{h}\right)^{0.4}25^{\left(\alpha\rho_s\frac{f_{yw}}{f_c}\right)} \times l \tag{6}$$

where γ_{el} is coefficient of primary and secondary elements, ω' and ω are mechanical steel ratio of compression and tension reinforcement, respectively, h is cross-section height, α is confinement effective factor, ρ_{sx} is confinement steel ratio, f_{yw} is yield strength of stirrup, and α_{st}, α_{cyc}, and α_{sl} are coefficients for type of steel, loading, and anchorage slip. For the yield strength of concrete components, the expression is given by Panagiotakos and Fardis [24]:

$$F_y = \frac{bd^3}{l}\phi_y\left\{E_c\frac{k_y^2}{2}\left(0.5(1+\delta') - \frac{k_y}{3}\right) + \frac{E_s}{2}\left[(1-k_y)\rho + (k_y-\delta')\rho' + \frac{\rho_v}{6}(1-\delta')\right]\right\}(1-\delta') \quad (7)$$

Conventionally, the damage index D can be obtained by using above expressions to obtain the nominal value of Park-Ang constants. Owing to limited statistical data and incomplete knowledge of mathematical model to predict these constants, the large convergence is reported as in [4–6, 23, 24]. Furthermore, these uncertainties will influence the quantification result of Park-Ang damage index. In order to verify the impact of damage quantification result derived from uncertainty of Park-Ang model constants, we present the structural performance database of PEER [25] to calibrate these constants and determine the uncertainty fluctuation range of each constant.

2.2. Comparison between the calibration results and empirical results

In this work, the calibration set is selected from the structural performance database of PEER and the selection criteria are such as (1) the cross section of column is rectangle; (2) the column is loaded cyclically until failure and the corresponding failure model is dominated by flexure; (3) the longitude bars in column should not be spliced and the column should experience more than two hysteretic cycles. In conformity with these criteria, 185 specimens are selected. Using these column load-displacement data, the performance points on the backbone curve of column under cyclic load are calibrated.

Similar to the most studies [23], the ultimate deformation under monotonic load δ_u is defined as a distinct reduction on the negative stiffness slope of backbone curve and 80% of maximum strength which is always assumed as F_u. Unfortunately, the missing monotonic load experiments oblige us to employ the statistical relationship of ultimate displacement under cyclic load and monotonic load to characterize the ultimate displacement. Herein, the failure displacement under typical load histories is assumed as 60% of their ultimate deformation capacity, which is firstly observed by Panagiotakos and Fardis [24]. For yield force, we defined that the value is 75% of the maximum force. Following above definitions, the energy coefficient β is computed with the assumption that damage index D is 1 at the ultimate state. In light with above definitions, the performance point is marked on the backbone of columns as depicted in **Figure 1**.

As shown in **Figure 1**, the column backbone curves are divided into two categories: one with obvious ultimate state point (the 80% maximum force) like in **Figure 1a**, the other with the largest displacement in backbone curve (e.g., **Figure 1b**). In order to yield the uncertainty distribution of empirical model, the attention is concentrated on the first category. Using the selected force-displacement data, the comparison of empirical model results and calibration results is given in **Figure 2**.

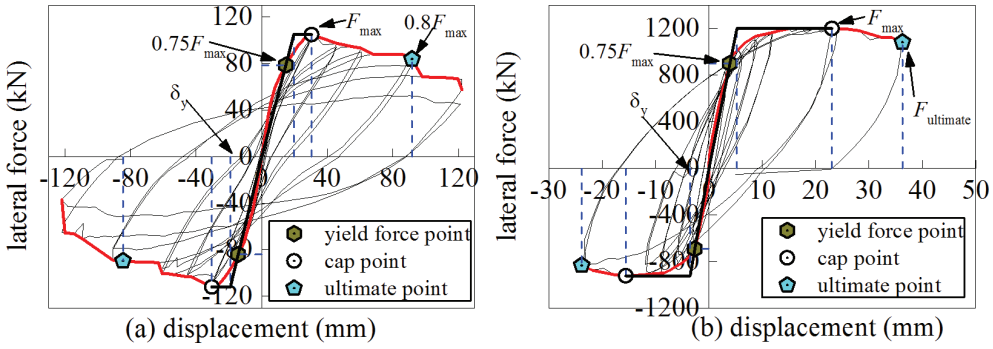

Figure 1. Performance point of backbone curve with obvious ultimate state point (a) and with the largest displacement point (b).

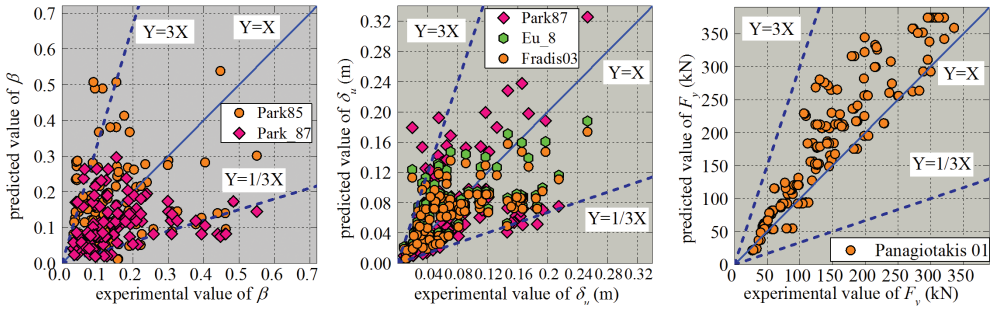

Figure 2. Comparison of predicted results and experimental results of β, δ_u and F_y.

As shown in **Figure 2**, the predicted and experimental values are scattered in a wide range, and this means the researchers should carefully handle the uncertainty derived from the empirical model in the process of evaluating damage state with Park-Ang model. Employing the parameter ε to represent the variability of predicted model deviation, the experimental value V_{exp} can be expressed as $V_{exp} = V_{pre} \times \varepsilon$. Taking into account the major fluctuation range of ε and the number of experimental samples, the ε which is located in the interval [1/3, 3] is selected and the range of data points which located less than 1/3 or more than 3 are discarded. In the light of above rules, the uncertainty source of β, δ_u, and F_y consists of 83, 111, and 173 specimen, respectively.

Along with classical concept, probability theory plays a key role in the UQ of physical model, and the distribution type is determined by the hypothesis test and related parameter are calibrated by enough experimental data. However, the limited data of experimental set and large variation restricted the ability of probability theory. As a generalized UQ measure, evidence theory is compatible with both aleatory and epistemic uncertainties. So, the evidence theory is adopted in this work to handle the epistemic uncertainty rooted in parameters of Park-Ang damage model.

http://dx.doi.org/10.5772/intechopen.68153

3. Evidence theory and differential evolution-based UQ for seismic damage assessment

3.1. Basic of the evidence theory

Evidence theory is a theoretical framework for reasoning with partial and unreliable information. It was proposed by Dempster [18] and further improved by Shafer [19]. Compared to the classical uncertain model theory, it offers the possibility to explicitly represent doubt and conflict. As the most basic concept of the evidence theory, the fame of discernment **Ω** is defined as a set of mutually exclusive elementary propositions. Due to limited information, the propositions can be scattered, nested, or partially overlapped. Thus, the mutually exclusive elementary propositions construct the power set $F = 2^{\Omega}$. Given the measureable sample space (Ω, *F*), the basic belief assignment (BBA) on *F*, *m* is a mapping $F \rightarrow$ [0, 1] that satisfies the following axioms:

$$m(A) \geq 0 \quad m(\varnothing) = 0 \quad \sum m(A) = 1 \quad \text{for each } A \subseteq \Omega \ . \tag{8}$$

An element A∈*F* for which $m(A) > 0$ is named a focal element. Corresponding to the scattered, nested, or partially overlapped propositions in *F*, it seems more reasonable to make use only of this available information to produce two uncertain measures, the Belief (*Bel*) and the Plausibility (*Pl*) functions (**Figure 3**).

Similar to the additive rule in probability, belief and plausibility measures of proposition A can be calculated from following formula:

$$Bel(A) = \sum\nolimits_{B \subseteq A} m(B) \quad \text{for all } B \subseteq 2^{\Omega} \tag{9}$$

$$Pl(A) = \sum\nolimits_{B \cap A \neq \varnothing} m(B) \quad \text{for all } B \subseteq 2^{\Omega} \tag{10}$$

where *A* represents different elements in *F*. In terms of two complementary sets *A* and $\tilde{A}$, the sum of belief and plausible function is not required to be one. But the weaker rule $Pl(A)+Bel(\tilde{A})=1$ is satisfied, and this expression is completely different from probability distribution function *p* in probability theory, that is, $p(A)+p(\tilde{A})=1$. As the most remarkable distinction from probability theory, evidence theory allows evidence stemming from different sources and employs the rules of combination to aggregate [26]. One of the most important combination rules is Dempster's rule which has following formulation. Given two independent BBA $m(B_1)$ and $m(B_2)$, the Dempster's rule can be expressed as:

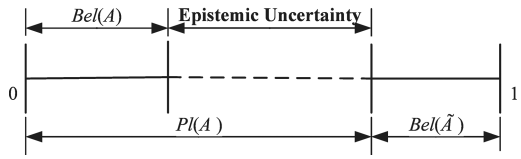

Figure 3. Belief function (*Bel*) and Plausibility function (*Pl*) of proposition A.

$$m(A) = \frac{\sum_{B_1 \cap B_2 = A} m(B_1)m(B_2)}{(1-K)} \quad \text{for all } A \neq \varnothing \tag{11}$$

where $K = \sum_{B_1 \cap B_2 = \varnothing} m(B_1)m(B_2)$ can be viewed as contradiction or conflict among the information given by the independent knowledge sources.

3.2. Evidence theory-based UQ of seismic damage assessment using differential evolution

3.2.1. Evidence-based uncertainty representation

For the purpose of UQ, the first step is the uncertainty representation of parameters using evidence theory, in which separate belief structures for each uncertain parameter should be constructed. In this work, we adopt a general methodology as described previously by Salehghaffari et al. [27] to obtain necessary information from available data and express the uncertain variables in the mathematical framework of evidence theory.

According to Salehghaffari et al. [27], two principle steps are involved in this methodology: (1) representation of uncertain parameters in several intervals through drawing bar charts by using all available data or directly from expert opinions and (2) identification of three relationships between all adjacent intervals and construction of the associated BBA structure. To further illustrate this, assuming that D_1 and D_2 represent the number of data points within two adjacent intervals I_1 and I_2, respectively, and $D_1 > D_2$, three relationships of two adjacent intervals can be identified as agreement $(D_2/D_1 \geq 0.8)$, conflict $(0.5 \leq D_2/D_1 < 0.8)$, and ignorance $(D_2/D_1 < 0.5)$ (see **Figure 4**), the corresponding belief structure and BBA value for these three relationships are calculated by Eqs. (12)–(14), respectively.

$$m(\{I\} = \{I_1, I_2\}) = (D_1 + D_2)/D_T \tag{12}$$

$$m(\{I_1\}) = D_1/D_T, \qquad m(\{I_2\}) = D_2/D_T \tag{13}$$

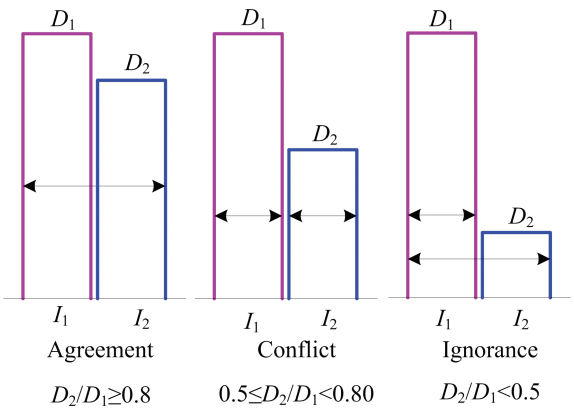

Figure 4. Three relationships of uncertain intervals.

$$m(\{I_1\}) = D_1/D_T, \qquad m(\{I_1, I_2\}) = D_2/D_T \tag{14}$$

where D_T denotes the total number of data points, following this approach, a reasonable BBA structure of uncertain parameter is constructed based on available data and knowledge, a more detailed illustration of uncertainty representation in intervals with assigned BBA value is referred in Salehghaffari et al. [27].

Employing this strategy, the uncertainty of Park-Ang model parameters can be properly represented with the evidence theory. In **Figure 5**, we use $\varepsilon_A(\beta)$, $\varepsilon_B(\beta)$, and $\varepsilon(F_y)$ to denote the variability of the predicted models in Refs. [4, 5] for energy constant β and the one in Ref. [24] for yielding force F_y of columns. The $\varepsilon_C(\delta_u)$, $\varepsilon_D(\delta_u)$, and $\varepsilon_E(\delta_u)$ in **Figure 6** represent the fluctuation of the empirical model for ultimate displacement under monotonic loading in Refs. [6, 22, 23].

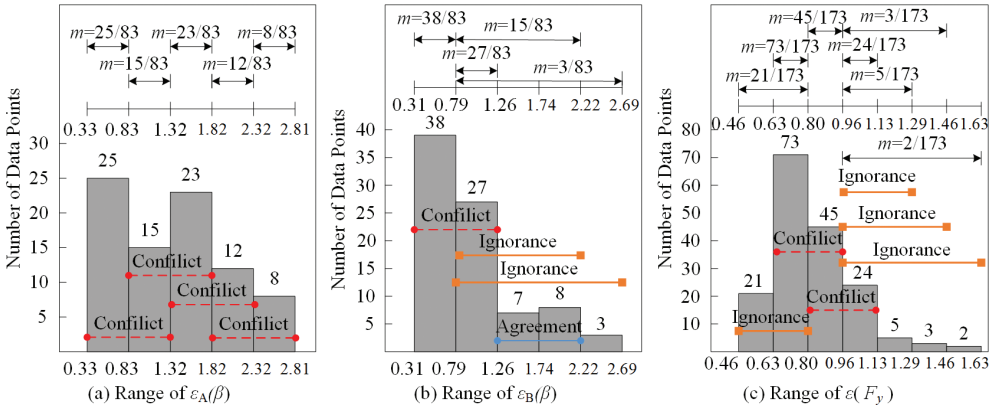

Figure 5. Evidential uncertainty description of $\varepsilon(\beta)$ and $\varepsilon(F_y)$.

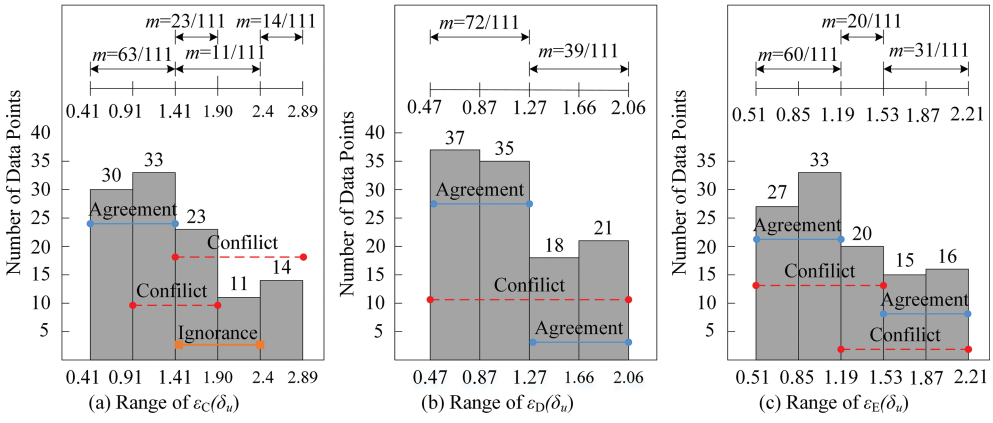

Figure 6. Evidential uncertainty description of $\varepsilon(\delta_u)$.

3.2.2. Uncertainty propagation using differential evolution

In evidence theory community, uncertainty variable is usually expressed to be a series of focal element intervals based on limited information and the joint frame of discernment is composed of the Cartesian products of uncertain intervals, then, the BBA value of each element of joint frame of discernment is also the Cartesian product of BBA value assigned on the corresponding interval. Given two independent uncertain parameters $u_1 \in \mathrm{U}_1$ and $u_2 \in \mathrm{U}_2$, and corresponding focal element C_1 and C_2, the joint BBA structure of this problem is defined as:

$$C{=}C_1 \otimes C_2, \qquad \forall u \in \mathrm{U}\ \forall u_1 \in \mathrm{U}_1\ \forall u_2 \in \mathrm{U}_2 \tag{15}$$

$$m(C) = m(C_1)m(C_2) \tag{16}$$

where the symbol $\otimes$ denotes the Cartesian products. Using Eqs. (15) and (16), the joint uncertainty input of system can be seemed as the multidimensional hypercube. Therefore, uncertainty propagation is a progress of finding the maximum and minimum of the system response value in each hypercube interval (proposition of the joint belief structure). To propagate the represented uncertainties of Park-Ang damage model constants, the damage index D is considered as system response.

Considering epistemic uncertainty of the system, the belief and plausibility functions of the response are obtained on the basis of the combined BBAs of the input parameters from different information sources using the evidence combination rules. For the prediction response process $D = f(Y)$, whose input parameter vector $\boldsymbol{Y} = (Y_1,\ldots,Y_n)$ has n variables with epistemic uncertainty, the joint proposition C of elementary proposition is constructed for the Park-Ang damage index prediction system model as:

$$C = \{c_k = [x_{1i_1}, x_{2i_2}, \cdots, x_{ni_n}] : x_{1i_1} \in \boldsymbol{X}_1, x_{2i_2} \in \boldsymbol{X}_2, \cdots, x_{ni_n} \in \boldsymbol{X}_n\} \tag{17}$$

where $\boldsymbol{X}_1$, $\boldsymbol{X}_2$, …, $\boldsymbol{X}_n$ denote the intervals sets (frame of discernment) of the n variables Y_1, Y_2, …, Y_n, and the relevant numbers of the intervals are $\boldsymbol{I}_1$, $\boldsymbol{I}_2$,…, $\boldsymbol{I}_n$. $x_{1i_1}, x_{2i_2}, \cdots, x_{ni_n}$ denote the subintervals, $0 \le ji_j \le I_j$ (j = 1,2,…,n); $\boldsymbol{c}_k$ denotes the n-dimensional joint proposition set constructed by several subintervals, and there are $\boldsymbol{I}_1, \boldsymbol{I}_2,\ldots,\boldsymbol{I}_n$ joint proposition sets $\boldsymbol{c}_k$ in C. The BBA of the joint proposition set C is defined as:

$$m_c(\boldsymbol{c}_k) = m_1(x_{1i_1})m_2(x_{2i_2})\cdots m_n(x_{ni_n}) \tag{18}$$

Thus every element of the Cartesian set C is required to be checked in the evaluation of the belief and plausibility functions by finding the system response bounds. That is to say the minimum and maximum responses of each joint set are needed to calculate:

$$[D_{\min}, D_{\max}] = [\min[f(c_k)], \max[f(c_k)]] \tag{19}$$

As uncertain variable is represented by many discontinuous set instead of smooth and continuous explicit function, time consuming is inevitable in UQ with evidence theory. There are two main approaches to find the bounds of the system response: sampling and optimization. The accuracy of sampling approach is highly dependent on the number of samples and the number of hypercubes, and the process is costly. On the contrary, optimization methods have the

potential to dramatically reduce the computational work. To alleviate this computational burden, based on authors' previous work [11], the differential evolution (DE) [28] optimization approach is used to calculate the response bounds of each hypercube and compute the composite BBA of each hypercube, propagation of the represented uncertainty through Park-Ang damage model (Eq. (1)). The characteristics of derivative-free and capability of handling discrete belief structure make DE method to be a good choice for such an interval bound task.

DE is arguably one of the most powerful stochastic real-parameter optimization algorithms for solving complex and computational optimization problems in current use. As a novel evolutionary computation technique, differential evolution resembles the structure of an evolutionary algorithm (EA). However, unlike traditional EAs, the DE-variants perturb the current generation population members with the scaled differences of randomly selected and distinct population members. The characteristics together with other factors of DE make it a fast and robust algorithm and as an alternative to EA. Since late 1990s, DE started to find several significant applications to the optimization problems arising from diverse domains of science and engineering. In a recently published article, Das and Suganthan [29] provided a comprehensive survey of the DE algorithm and its basic concepts, different structures and variants for solving various optimization problems, as well as applications of DE variants to practical optimization problems.

In the context of DE, the individual trial solutions (which constitute a population) are called parameter vectors or genomes. Let $S \in R_n$ be the search space of the problem. Then, the n-dimensional vector can be represented by $\boldsymbol{x}_i = (x_{i1}, x_{i2}, \ldots, x_{in})^T \in S$, $i = 1, 2, \ldots, NP$, and DE algorithm utilizes NP as a population for each iteration, called a generation of the algorithm. For the damage index assessment response process, its parameter vector is generated by the uncertainty variables (β, F_y, and δ_u) in ranges according to their respective belief structures. DE operates through the same computational steps as employed by a standard EA, including crossover, mutation, crossover, and selection operators, but differs from traditional EAs, DE employs difference of the parameter vectors to explore the objective function landscape. As above brief description, the pseudocode of DE is presented in **Figure 7** and with a detailed survey of the DE family of algorithms can be found in Ref. [29].

Take the pseudocode of DE in mind, the illustration of DE-based computational strategy for finding the propagated belief structure by the example as shown in **Figure 8** (only one uncertain parameter is considered).

The procedure of uncertainty propagation using the DE strategy is as follows:

- Collect all uncertain information and construct corresponding BBA structure of each uncertain parameter, combine the BBA structures under the situation of evidences provided by different sources or experts using combination rules of evidence.
- Use differential evolution algorithm to calculate the bound values of the system response within each joint interval and construct corresponding joint belief structures.
- Given the complete BBA on the output response of interest damage index D, the belief and plausibility functions on D are given and any general subset can be developed by applying Eqs. (9) and (10).

Step1: Set the values of mutation constants F, crossover constants CR, population size NP, maximum numbers of generations G_{max}, object function $f()$ and number of parameters of object function ID

Step 2: Randomly initialize the NP population $\boldsymbol{x}_i^0$ (i<=NP) and select the best competitor $\boldsymbol{x}_{best}^0$

Step3: WHILE G<=G_{max} or convergency criterion is not satisfied

FOR i=1 to NP

***3.1 Mutation step*:** the mutated vector is generated as

$$v_i^{G+1} = x_i^G + F_1\left(x_{best}^G - x_i^G\right) + F\left(x_{r1}^G - x_{r2}^G\right)$$

***3.2 Cross step*:** for each mutated vector, the trial vector is generated using

FOR j=1 to ID

IF rand(j)≤CR or j=randn(i) THEN $u_{ij}^{G+1} = v_{ij}^{G+1}$

OTHERWISE $u_{ij}^{G+1} = x_{ij}^{G+1}$

END IF

END FOR

3.3 Selection step: Evaluate each trial vector $u_i^{(G+1)}$

IF $f(u_i^{G+!}) < f\left(x_i^{G+1}\right)$ THEN $x_i^{G+1} = u_i^{G+1}$

OTHERWISE $x_i^{G+1} = x_i^G$

IF $f(x_i^{G+!}) < f\left(x_{best}^G\right)$ THEN $x_{best}^{G+1} = x_i^{G+1}$

OTHERWISE $x_{best}^{G+1} = x_{best}^G$

END IF

END IF

END FOR

3.4 Increment the generation count G=G+1

END WHILE

Figure 7. Pseudocode of DE.

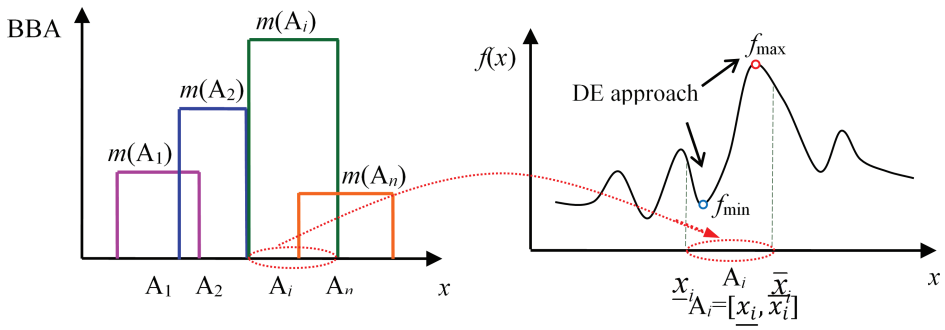

Figure 8. Uncertainty propagation of belief structure of system by DE.

Once the BBA structure of the Park-Ang damage index response is constructed, observed evidence on simulation responses is used in the determination of target propositions to

estimate uncertainty measures, i.e., cumulative belief function (CBF) and cumulative plausibility function (CPF).

3.2.3. Uncertainty measurement for seismic damage assessment

In evidence theory framework, the plausibility function *Pl* and belief function *Bel* are used to denote the uncertainty measurement. Employing the construction rule proposed by Sentz et al. [30], the CBF and CPF of Park-Ang damage index D less than the threshold value are formulated as follows:

$$Pl(D_{\text{thre}}) = \sum_{u_D \cap U_D \neq \varnothing} m(u) \quad U_D = \{u_D \leq D_{\text{thre}}\} \tag{20}$$

$$Bel(D_{\text{thre}}) = \sum_{u_D \subseteq U_D} m(u) \quad U_D = \{u_D \leq D_{\text{thre}}\} \tag{21}$$

Where $u_D \cap U_D \neq \varnothing$ means that the joint focal element u can be entirely or partially within the threshold domain $u_D \leq D_{\text{thre}}$ and $u_D \subseteq U_D$ means that the joint focal element u_D can be entirely within the threshold domain $u_D \leq D_{\text{thre}}$. Summarized above subparts, the separate stages of UQ framework of evidence theory using differential evolution optimization is shown in **Figure 9**.

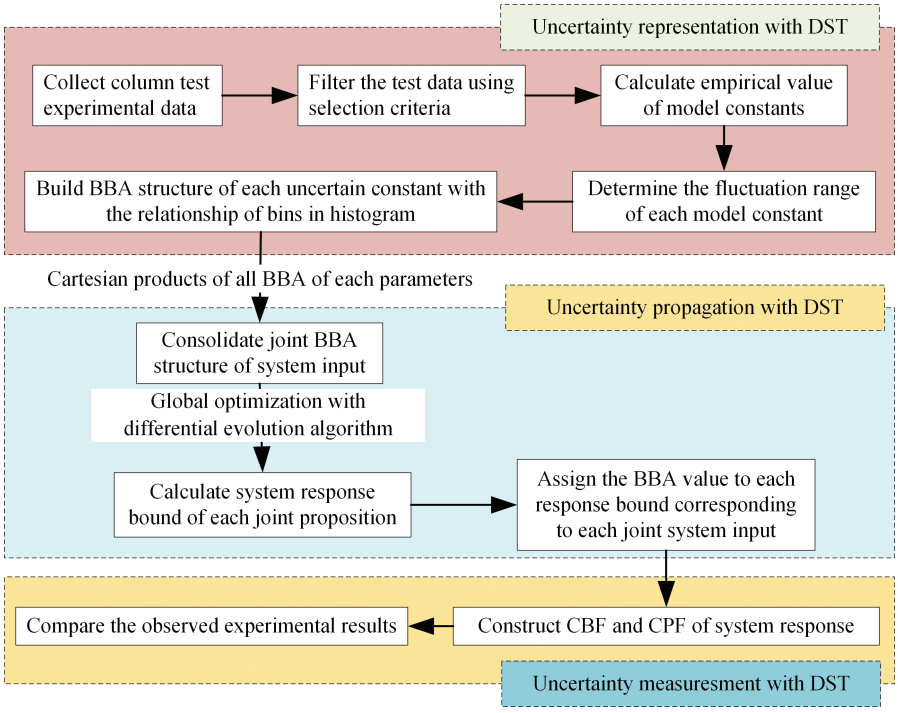

Figure 9. Procedure of UQ of Park-Ang damage model.

4. Case study

In order to investigate the effectiveness and feasibility of the proposed UQ measures, the column "zahn86u7" [31] is selected to compute the Park-Ang damage index in its load step. The backbone curve and load history are shown in **Figure 10**.

As shown in **Figure 10a**, the ultimate cyclic displacement is calibrated by using the average value of 80% maximum force point on the force capacity reduction slope of positive and negative direction. The effective path in **Figure 10b** denotes the load path from initial state to ultimate state and the load path is the global displacement history. Using the properties of column, listed in the webpage of PEER, the nominal value of constants in Park-Ang damage model β, δ_u and F_y can be estimated by the empirical expressions from Eq. (2) to Eq. (7), respectively. In consistent with Section 3.2, the uncertainty distribution of model constants can be depicted as the nominal value multiply the factor ε. Taking the computed results into the evidence representation process, the BBA structures of β, δ_u, and F_y with different models are listed in **Tables 1** and **2**.

Taking above uncertain information into the differential evolution-based uncertainty propagation framework, the evidential UQ results for each load step as shown in **Figure 11**.

To validate the generality of evidence theory, the variability of Park-Ang model parameters is also represented by probability theory. The goodness of fit test is applied to test the distribution type and determine the related distribution parameters. The uncertainty distribution information of model B for β model C for δ_u and F_y is presented in **Table 3**.

From **Table 3**, the values of $\varepsilon(\beta)$ and $\varepsilon(\delta_u)$ do not refuse the normal and lognormal distribution. We use two strategies to construct the probability input of variables. In first strategy, the lognormal distribution is applied to fit all the uncertainty inputs and the cumulative distribution

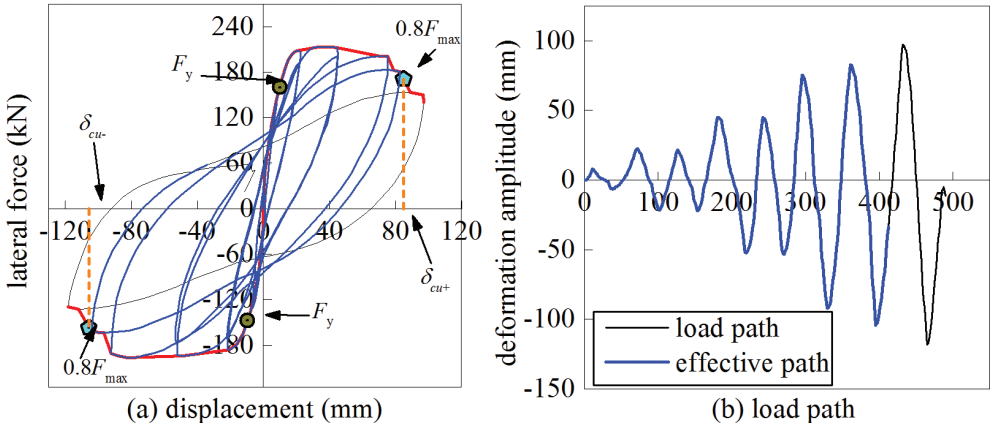

Figure 10. Backbone curve (a) and load path (b) of columns of column test.

β				F_y	
Model A		**Model B**			
Range	**BBA**	**Range**	**BBA**	**Range**	**BBA**
[0.0345, 0.087]	0.301	[0.0266, 0.067]	0.458	[77.40, 133.19]	0.121
[0.0873, 0.139]	0.181	[0.0672, 0.108]	0.325	[105.22, 133.19]	0.422
[0.139, 0.192]	0.277	[0.0672, 0.189]	0.181	[133.19, 161.01]	0.26
[0.192, 0.244]	0.145	[0.0672, 0.230]	0.036	[161.01, 188.82]	0.139
[0.244, 0.296]	0.096			[161.0, 216.63]	0.029
				[161.01, 244.44]	0.017
				[161.01, 272.42]	0.012

Table 1. The BBA structure for multisource of β and F_y.

Model C		**Model D**		**Model E**	
Range	**BBA**	**Range**	**BBA**	**Range**	**BBA**
[0.034, 0.115]	0.568	[0.043, 0.116]	0.649	[0.0442, 0.104]	0.541
[0.115, 0.156]	0.207	[0.116, 0.188]	0.351	[0.104, 0.133]	0.180
[0.115, 0.196]	0.01			[0.133, 0.193]	0.279
[0.196, 0.237]	0.125				

Table 2. The BBA structure for multisource of δ_u.

function of uncertainty response which is indicated as CDF1. In other strategy, the probability distributions of $\varepsilon(\beta)$ and $\varepsilon(\delta_u)$ are assigned as normal distribution, while the distribution of $\varepsilon(F_y)$ is lognormal and corresponding cumulative distribution function of uncertainty result is represented as CDF2. To compare the quantification results of probability and evidence theory, **Figure 12** is presented to describe the damage index evolution in load steps 280 and 412, respectively. To make a further illustration for the damage state evolution in each load step, the point 0.25, 0.5, 0.75, and 1 are used to represent the minor, moderate, severe, and collapse damage state, respectively.

As illustrated in **Figure 12**, the probability theory based UQ results CDF1 and CDF2 are located in the range of curves CPF and CBF, this indicates that evidence theory is compatible to probability theory. The discrepancy of CDF1 and CDF2 demonstrates that probability theory may not be suitable to handle the epistemic uncertainty which is stemmed from limited experimental data. In other words, the probabilistic UQ result is ambiguous due to epistemic uncertainty and the choice of distribution type has a great impact on the quantification result. However, evidential UQ strategy demonstrates its power to quantify the epistemic uncertainty

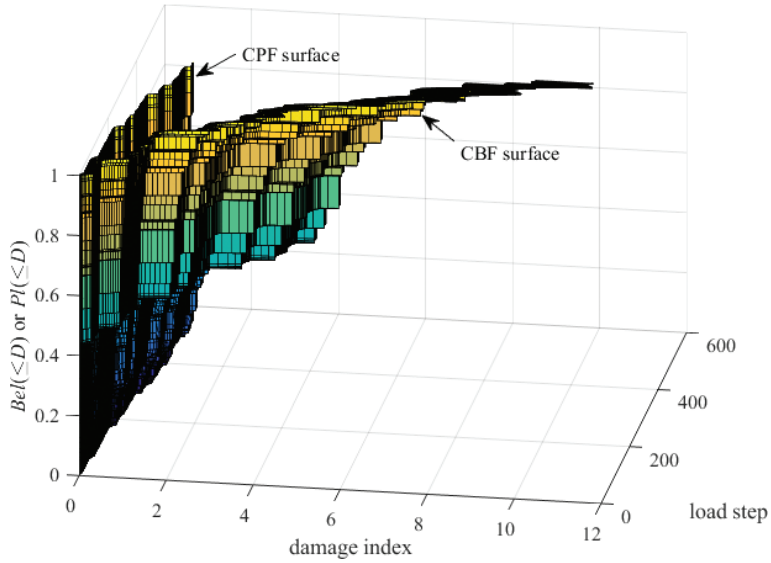

Figure 11. The evidential uncertainty propagation results of Park-Ang damage index.

Constants	Distribution type	m_u	σ
$\varepsilon_B(\beta)$	Normal	0.963	0.529
	Lognormal	-0.171	0.514
$\varepsilon_C(\delta_u)$	Normal	1.404	0.697
	Lognormal	0.206	0.537
$\varepsilon(F_y)$	Lognormal	-0.272	0.225

Table 3. The distribution information of Park-Ang constants.

because of its two uncertain measures belief function and plausibility function. In order to further clarify the influence of epistemic uncertainty, the quantitative results of damage index in **Figures 12a** and **b** are reported in **Table 4**.

As shown in **Table 4**, the belief interval of moderate damage state in steps 280 and 412 are [0.11, 0.447] and [0, 0.026], respectively. This means the exceeding probability of moderate damage state are [0.553, 0.89] and [0.974, 1] in steps 280 and 412, respectively. **Table 5** also displays the cumulative distribution value for moderate damage state for probability-theory-based quantification results. Using the first probability strategy CDF1, the cumulative distribution for moderate damage state are 0.217 and 0 corresponding to steps 280 and step 412. This means the exceeding probabilities of moderate damage state are 0.783 and 1 in steps 280 and 412, respectively. Analogously, the cumulative distribution values of CDF2 for moderate damage state are 0.298 and 0 in steps 280 and 412, respectively. It is worth noting the divergence of the cumulative distribution values of CDF1 and CDF2 in step 280. Furthermore, the

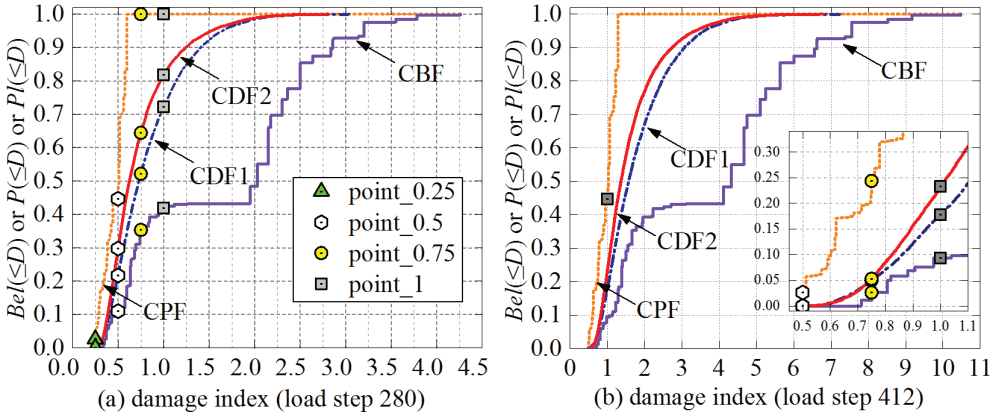

Figure 12. Comparison of propagation results using evidence theory and probability theory. (a) The cumulative distribution of damage index in step 280 and (b) the cumulative distribution of damage index in step 412.

Damage index	Cumulative distribution curve in step 280				Damage index	Cumulative distribution curve in step 412			
	CPF	CDF1	CDF2	CBF		CPF	CDF1	CDF2	CBF
0.25	0.026	0	0	0	0.25	0	0	0	0
0.5	0.447	0.217	0.298	0.11	0.5	0.026	0	0	0
0.75	1	0.522	0.644	0.354	0.75	0.244	0.050	0.053	0.026
1	1	0.722	0.818	0.419	1	0.447	0.178	0.233	0.094

Table 4. The cumulative distribution value of Park-Ang constants in step 280 and 412.

divergence of two kind probability-based quantification results provides the evidence that probability theory is not able to handle the epistemic uncertainty. Comparing the quantification results of collapse damage state, the similar conclusion can be obtained. Especially, the cumulative distribution value for collapse damage state is step 412, the evidence result is [0.094, 0.447], this means the value of damage index larger than 1 is located in the interval [0.453, 0.906]. While the cumulative probabilities of CDF1 and CDF2 are 0.178 and 0.233, respectively. This illustrates that the exceedance probability of collapse state is 0.822 for CDF1 and 0.767 for CDF2. From the view of risk assessment, the evidence theory will give decision maker a more robust UQ result, but the probability cannot.

With the incomplete knowledge of prediction model under the various operation conditions, different expert evidence conflicts are inevitable. To reconcile this task challenge, evidence combination rule is proposed to combine the evidences from multisource. Herein, the Dempster's rule is applied to aggregate the different source of evidence for β, δ_u, and F_y as shown in **Table 5**.

Using the aggregated BBA structures of these three uncertain parameters, the system uncertain response CPF2 and CBF2 are shown in **Figure 13**. To clarify the effectiveness of combination

β		δ_u		F_y	
Range	**BBA**	**Range**	**BBA**	**Range**	**BBA**
[0.035, 0.067]	0.297	[0.044, 0.104]	0.568	[77.40, 133.19]	0.121
[0.067, 0.087]	0.351	[0.104, 0.115]	0.189	[105.22, 133.19]	0.422
[0.087, 0.108]	0.127	[0.115, 0.116]	0.102	[133.19, 161.01]	0.26
[0.087, 0.139]	0.085	[0.116, 0.133]	0.055	[161.01, 188.82]	0.139
[0.139, 0.189]	0.108	[0.133, 0.156]	0.058	[161.01, 216.63]	0.029
[0.139, 0.192]	0.021	[0.133, 0.188]	0.028	[161.01, 244.44]	0.017
[0.192, 0.230]	0.011			[161.01, 272.42]	0.012

Table 5. The combined BBA structure for β, δ_u, and F_y.

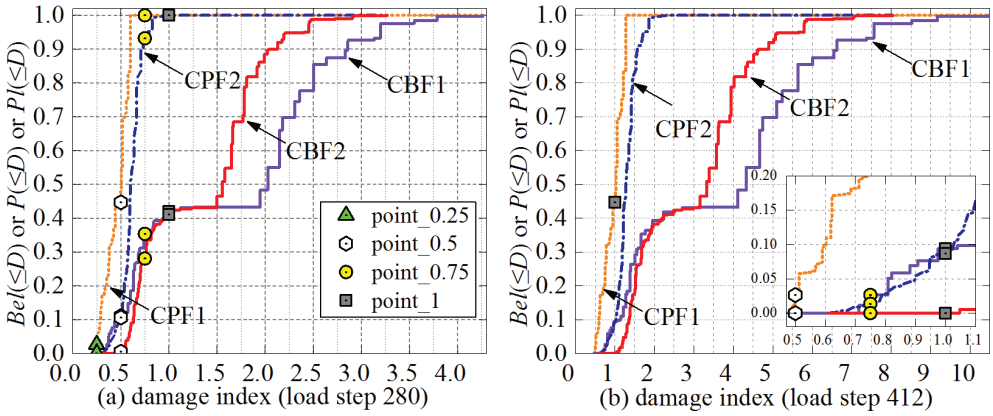

Figure 13. Comparison of propagation results with uncombined and combined BBA input. (a) The cumulative distribution of damage index in step 280 and (b) the cumulative distribution of damage index in step 412.

rule, the uncertainty propagation results CPF1 and CBF1 from the model B of β and model C of δ_u and F_y are also listed in **Figure 13**.

As shown in **Figure 13**, the UQ results of Park-Ang damage index variate in a large range. The distance of CBF and CPF denotes the epistemic uncertainty that is derived from the limited experimental data and lack of knowledge for complicated composite materials (e.g., parameters model hypothesis, material properties) or incomplete knowledge of empirical model. In comparison with the distance of CPF1 and CBF1 for uncombined BBA, the distance of CPF2 and CBF2 for combined BBA is much narrower, and this can be explained as the high conflict information of multisources that are discarded by aggregating the multisources evidence. However, the aggregation rule is not established in probability theory. From this point of view, the evidence theory has great potential to quantify the uncertainty from multisources which are having great existence in civil engineering.

5. Conclusions

UQ of seismic damage model are important for PBSD and performance-based seismic assessment. In this chapter, the epistemic uncertainty of the constants of Park-Ang model is taken into account. The Park-Ang damage model constants are calibrated with column set, selected from PEER column performance database. To effectively represent the uncertainty inherent in Park-Ang model constants with limited experimental data, the UQ measurement that combines evidence theory and differential evolution is presented. In order to further investigate the feasibility and effectiveness of presented UQ measurement, the Monte-Carlo sampling method combined with classical probability distribution, which is fitted with given data, is used. Comparing the propagation results of evidence theory and classical probability theory, we can conclude that the evidence theory is flexible to handle the epistemic uncertainty, which is stemmed from lack of knowledge or sparse experimental data, whereas the classical probability theory may be limited by the selection of distribution type and the determination of value for the distribution parameters. Using the aggregation rules of evidence theory demonstrates that evidence theory is capable to handle the uncertainty from multisources.

Acknowledgements

This study was supported by the Ministry of Science and Technology of China, Grant No. SLDRCE14-B-03 and the National Natural Science Foundation of China, Grant Nos. 51178337 and 51478356.

Author details

Hesheng Tang*, Dawei Li and Songtao Xue

*Address all correspondence to: 02036@tongji.edu.cn

State Key Laboratory for Disaster Reduction in Civil Engineering, Tongji University, Shanghai, China

References

[1] ASCE. ASCE Standard ASCE/SEI41-06: Seismic Rehabilitation of Existing Buildings. American Society of Civil Engineers: Reston, Virginia; 2007

[2] Krätzig WB, Meyer IF, Meskouris K, editors. Damage evolution in reinforced concrete members under cyclic loading. Proceedings of 5th International Conference on Structural Safety and Reliability, San Francisco; 1989:795–804

[3] Teran-Gilmore A, Avila E, Rangel G. On the use of plastic energy to establish strength requirements in ductile structures. Engineering Structures. 2003;**25**(7):965–80

[4] Park YJ, Ang AHS. Mechanistic seismic damage model for reinforced concrete. Journal of Structural Engineering. 1985;**111**(4):722–39

[5] Kunnath S, Reinhorn A, Park Y. Analytical modeling of inelastic seismic response of R/C structures. Journal of Structural Engineering. 1990;**116**(4):996–1017

[6] Park YJ, Ang AHS, Wen YK. Damage-limiting aseismic design of buildings. Earthquake Spectra. 1987;**3**(1):1–26

[7] Park Y-J, Ang AHS, Wen YK. Seismic damage analysis of reinforced concrete buildings. Journal of Structural Engineering. 1985;**111**(4):740–57

[8] Fajfar P. Equivalent ductility factors, taking into account low-cycle fatigue. Earthquake Engineering & Structural Dynamics. 1992;**21**(10):837–48

[9] Chai YH, Romstad KM, Bird SM. Energy-based linear damage model for high-intensity seismic loading. Journal of Structural Engineering. 1995;**121**(5):857–64

[10] Rajabi R, Barghi M, Rajabi R. Investigation of Park-Ang damage index model for flexural behavior of reinforced concrete columns. The Structural Design of Tall and Special Buildings. 2013;**22**(17):1350–1358

[11] Tang HS, Li DW, editors. Uncertainty quantification of the Park-Ang damage model applied to performance based design. Proceedings of the Fifteenth International Conference on Civil, Structural and Environmental Engineering Computing. Stirling shire, UK: Civil-Comp Press; 2015; 170–170.

[12] Williams MS, Sexsmith RG. Seismic assessment of concrete bridges using inelastic damage analysis. Engineering Structures. 1997;**19**(3):208–16

[13] Williams MS, Sexsmith RG. Seismic damage indices for concrete structures: A state-of--the-art review. Earthquake Spectra. 1995;**11**(2):319–49

[14] Zadeh LA. Fuzzy sets. Information and Control. 1965;**8**(3):338–53

[15] Dubois D, Prade HM, Farreny H, Martin-Clouaire R, Testemale C. Possibility theory: An Approach to Computerized Processing of Uncertainty. New York: Plenum press; 1988

[16] Moore RE. Interval Analysis. Englewood Cliffs: Prentice-Hall; 1966.

[17] Walley P. Statistical Reasoning with Imprecise Probabilities. London: Chapman and Hall; 1991

[18] Dempster AP. Upper and lower probabilities induced by a multivalued mapping. The Annals of Mathematical Statistics. 1967;**38**(2):325–39

[19] Shafer G. A Mathematical Theory of Evidence. Princeton: Princeton University Press; 1976

[20] Tang H, Su Y, Wang J. Evidence theory and differential evolution based uncertainty quantification for buckling load of semi-rigid jointed frames. Sadhana. 2015;**40**(5):1611–27

[21] Oberkampf WL, Helton JC, Sentz K, editors. Mathematical Representation of Uncertainty. Non-Deterministic Approaches Forum. American Institute of Aeronautics and Astronautics Seattle, WA, Paper; 2001.

[22] CEN. Eurocode 8: Design of Structures for Earthquake Resistance-Part 3: Assessment and Retrofitting of Buildings; European Committee for Standardization 2005.

[23] Fardis MN, Biskinis DE, editors. Deformation capacity of RC members, as controlled by flexure or shear. Proceedings of International Symposium on Performance-based Engineering for Earthquake Resistant Structures honoring Prof. Shunsuke Otani, University of Tokyo; 2003: 511–530.

[24] Panagiotakos TB, Fardis MN. Deformations of reinforced concrete members at yielding and ultimate. ACI Structural Journal. 2001; **98**(2): 135–148.

[25] University of Washington. The UW-PEER Reinforced Concrete Column Test Database Washington [Internet] 2004 [Available from: http://www.ce.washington.edu/peera1/

[26] Sentz K, Ferson S. Combination of evidence in Dempster-Shafer theory. Callaos N, Ebisuzaki T, Starr B, Abe JM, Lichtblau D, editors. Orlando: International Institute Informatics & Systemics; 2002

[27] Salehgh affari S, Rais-Rohani M, Marin EB, Bammann DJ. A new approach for determination of material constants of internal state variable based plasticity models and their uncertainty quantification. Computational Materials Science. 2012;**55**:237–44.

[28] Storn R, Price K. Differential evolution–a simple and efficient heuristic for global optimization over continuous spaces. Journal of Global optimization. 1997;**11**(4):341–59

[29] Das S, Suganthan PN. Differential evolution: a survey of the state-of-the-art. Evolutionary Computation, IEEE Transactions on. 2011;**15**(1):4–31

[30] Ferson S, Kreinovick V, Ginzburg L, Sentz F. Constructing Probability Boxes and Dempster-Shafer Structures. United States, Albuquerque, NM (US); Livermore, CA (US): Sandia National Labs; 2003. Contract No: SAND2002-4015

[31] Zahn FA. Design of Reinforced Concrete Bridge Columns for Strength and Ductility. University of Canterbury; 1985